

Experimental Section

Materials. All reagents were acquired from Aldrich Chemical Co. unless otherwise noted. PMP (TPX X22, Mitsui Plastics) was purchased as 50 μm thick film and used as received. The PMP was determined to be a copolymer of 4-methyl-1-pentene and a linear monomer believed to be 1-octene (~ 3 mol %) by NMR analysis. For mass uptake experiments, a 2 mm PMP coupon (TPX RT18, Mitsui Plastics) was used and was found to be a copolymer with the same comonomer as the film sample although in a smaller concentration (<1 mol %). MAH was recrystallized twice from chloroform. Benzoyl peroxide (BPO) and dicumyl peroxide (DCP) were found to be $>97\%$ pure by NMR and were used as received. Carbon dioxide (Coleman grade 99.99%, Merriam Graves) was passed through activated alumina and Q-5 catalyst (Englehard Industries) to ensure purity throughout our system by removing water and oxygen, respectively. Carbon tetrachloride and acetone (HPLC Grade, Fisher) were used as received. Commercial samples of maleated polyethylenes were obtained from Quantum Chemical Company (PX-360) and DuPont Canada (Fusabond "E"-MB 226D).

Phase Behavior. A determination of phase behavior was made visually by using a 316 stainless steel view cell (3 in. long \times $1\frac{1}{16}$ in. i.d.) with a volume of 14 mL. The cell is sealed on each end with Teflon O-rings and 1 in. diameter sapphire windows. Brass rings are used on the external side of the windows to protect the sapphire from the stainless steel end caps. The cell is fitted with an aluminum jacket with $\frac{1}{4}$ in. diameter cartridge heaters used for temperature control. A 100DM high-pressure syringe pump (Isco) fitted with a heating/cooling jacket delivers the CO_2 into the vessel.

Maleations. Reactions were run in 316 stainless steel, high-pressure reaction vessels that were machined from $\frac{7}{8}$ in. hexagonal stock (4 in. long \times $\frac{7}{16}$ in. i.d.). The vessels, tapped with $\frac{1}{4}$ in. NPT threads, were plugged on one end and fitted with an $\frac{1}{8}$ in. high-pressure needle valve on the other, giving the vessels a total volume of approximately 8 mL each. The vessels were charged with PMP (0.40 g), maleic anhydride (0.2 or 0.05 g), and either BPO (0.08 g) or DCP (0.09 g), purged with nitrogen, and heated to 60 $^\circ\text{C}$ before adding SC CO_2 (~ 5.4 g) via the Isco pump. The vessels were soaked at 60 $^\circ\text{C}$ for 4 h prior to heating to the reaction temperature of 125 $^\circ\text{C}$ in the case of the BPO-initiated experiments to allow for equilibration of the reagents into the PMP film. For the DCP-initiated reactions, the vessels were immediately heated to 125 $^\circ\text{C}$ after filling. At the end of the reaction period, the vessels were quenched under cold, running water, and the pressure was released into the hood. The samples were rinsed in acetone for ~ 5 min to remove unreacted reagents. (A 24 h soak in refluxing acetone yielded the same result.) Variations of this procedure were employed to better understand the reaction. These included varying the amount of maleic anhydride (0.005–0.5 g), BPO (0.026–0.26 g), DCP (0.025–0.11 g), or CO_2 (3.0–6.0 g) as well as varying the reaction time (0–24 h) and the reaction temperature (60–135 $^\circ\text{C}$).

Characterization. Transmission and attenuated total reflectance (ATR) infrared spectroscopic experiments were conducted using a Bio-Rad 175C FTIR. Direct transmission analyses of the 50 μm films were run on the PMP and grafted samples. A 45 $^\circ$ germanium internal reflection element was used for the ATR IR measurements. Differential scanning calorimetry (DSC) measurements were conducted on a DuPont 2000 DSC under nitrogen flow at a heating rate of 10 $^\circ\text{C}/\text{min}$. The heat of fusion value used in calculations of PMP crystallinity was 61.7 J/g.¹⁵ Thermal gravimetric analysis (TGA) was carried out with a DuPont Instruments TGA 2950 at a heating rate of 10 $^\circ\text{C}/\text{min}$ to 480 $^\circ\text{C}$ under nitrogen. Elemental analyses were performed by Galbraith Laboratories. ^{13}C NMR analysis of the virgin PMP was conducted on a Bruker 500 MHz NMR at 50 $^\circ\text{C}$ using carbon tetrachloride and 5% *p*-xylene- d_{10} as the solvent. Reagent purity was determined in acetone- d_6 by utilizing ^1H - and ^{13}C NMR spectra obtained with a Bruker 300 MHz NMR. For X-ray analysis, an evacuated Statton camera operating with Ni-filtered $\text{Cu K}\alpha$

radiation was used. The wavelength of the radiation is 1.5418 \AA , and the camera length used was 4.89 cm.

Mass Uptake Experiments. The determination of CO_2 solubility in PMP under conditions similar to that of the reaction was conducted according to the work of Berens.¹⁶ PMP samples weighing approximately 1 g were cut from the 2 mm thick coupon. The samples were placed in high-pressure reaction vessels, heated to 60 $^\circ\text{C}$, and pressurized to 180 atm (0.68 g/mL) CO_2 . After a given soak period, the samples were quickly removed from the vessels and placed on a balance interfaced to a computer. The mass loss (CO_2 desorption) was recorded as a function of time.

Swelling Experiments. Grafted samples (~ 50 mg) were soaked in 5 mL of carbon tetrachloride for 1 h at 60 $^\circ\text{C}$. The gels were removed from the solutions, placed in tared vials and weighed. The gels were then dried in vacuo and weighed once again. The degree of swelling was calculated as the mass of solvent per mass of polymer (g/g) in the gel.

Results and Discussion

Before the maleation reaction in SC CO_2 was investigated, the phase behavior of the system was examined, including the solubility of the reactants in SC CO_2 , the carbon dioxide in the substrate, and the reactants in the fluid-swollen PMP. As reported earlier by Paulaitis,¹⁷ maleic anhydride is completely miscible with SC CO_2 at conditions slightly higher than the critical point of the fluid alone having an upper critical end-point (UCEP) of 35.8 $^\circ\text{C}$ and 78.0 atm. The phase diagram which they report, however, corresponds only to dilute solutions. Even at the highest concentration of maleic anhydride used in our studies (0.5 M), the solution is homogeneous at the reaction temperature of 125 $^\circ\text{C}$ and pressure of 400 atm, but the cloud point is significantly higher on the pressure–temperature scale (85 $^\circ\text{C}$, 240 atm) than the UCEP reported by Paulaitis. BPO forms a biphasic mixture with CO_2 under the conditions used for filling (60 $^\circ\text{C}$, 180 atm) but slowly equilibrates to a nearly homogeneous system during the soaking period of 4 h. Upon further heating, the BPO forms a homogeneous solution during the final stages of the temperature/pressure ramp. DCP forms a homogeneous solution in SC CO_2 at all temperatures and pressures examined. Because of these differences in the phase behavior of the two initiators, it was necessary to employ a soak period for the BPO reactions to accommodate the slow equilibration while in most cases the DCP reactions were immediately heated to the reaction temperature after filling. Soaking at 60 $^\circ\text{C}$ for up to 48 h was not found to initiate a maleation reaction; therefore, this difference in the treatment of initiators was not expected to create any discrepancies in the comparison of data.

Carbon dioxide uptake experiments were conducted to determine the kinetics of CO_2 absorption and the equilibrium sorbed mass in PMP under our reaction conditions. Figure 1a shows the results of these experiments conducted at 60 $^\circ\text{C}$ and 180 atm over 6 h. The equilibrium mass uptake was found to be 17.6% and the diffusion coefficient is estimated as $\sim 5.4 \times 10^{-5} \text{ cm}^2/\text{s}$, from the initial slope of a plot of M_t/M_{inf} vs $t^{1/2}/\lambda$ where M_t is the mass of CO_2 absorbed at time t , M_{inf} is the equilibrium mass absorbed, and λ is the sample thickness.¹⁸ Other semicrystalline polymers studied in our labs (high-density polyethylene,⁴ poly(chlorotrifluoroethylene)², and poly(tetrafluoroethylene)⁵) have CO_2 mass uptakes of 3–4% and diffusivities on the order of 10^{-6} – $10^{-8} \text{ cm}^2/\text{s}$ under similar conditions. PMP is capable of swelling quickly and significantly with carbon dioxide. Attempts were made to measure the solubility

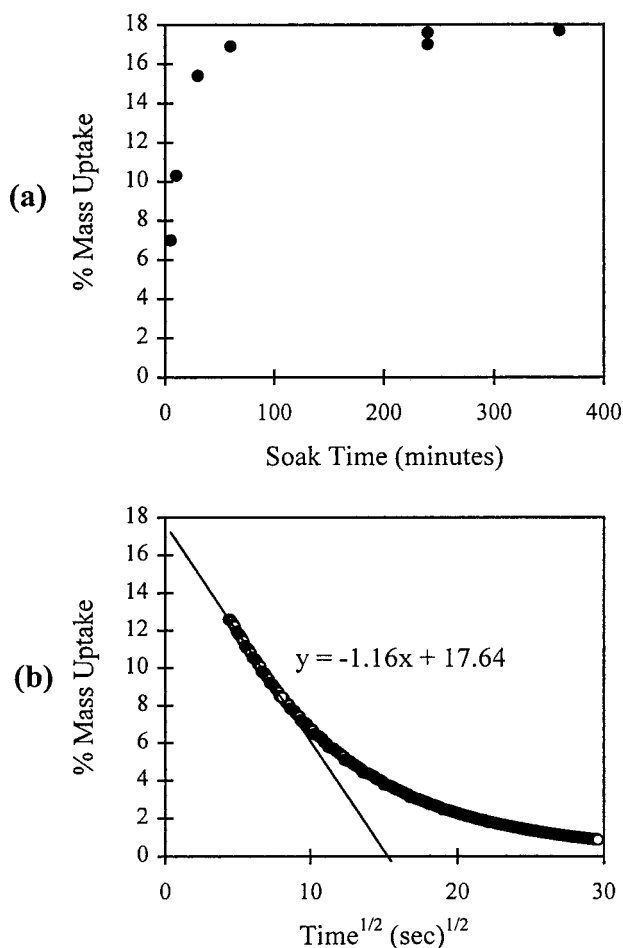


Figure 1. (a) Kinetics of CO₂ uptake in PMP at 60 °C, 180 atm. (b) Representative desorption profile (4 h soak at 60 °C, 180 atm).

of CO₂ in PMP at 125 °C, but desorption was too fast to measure.

A representative CO₂ desorption curve is shown in Figure 1b (representing the 4 h desorption point in Figure 1a). We assume that the initial linearity of the mass loss as a function of the square root of time indicates Fickian kinetics for desorption of CO₂ from PMP, but the curvature at longer times is pronounced and likely indicates non-Fickian behavior after the initial desorption period. According to Puleo,¹⁹ CO₂ is soluble in the crystalline domains and diffuses from these regions at a lower rate; thus, we expect that some of the curvature results from a combination of the diffusion from both the amorphous and crystalline regimes.

MAH solubility in the fluid-swollen PMP was measured gravimetrically with TGA after exposure of a PMP sample to typical MAH concentrations in SC CO₂ at 60 °C. The resulting uptake values of 0.4 wt % were 1 order of magnitude below the expected values based on the grafting experiments (see below). We ascribe this discrepancy to two factors: (1) a difference in partitioning of the reagent at the higher reaction temperature of 125 °C compared to the measurement temperature of 60 °C and (2) the desorption of maleic anhydride from PMP during depressurization. Uptake measurements conducted at higher temperatures yielded slightly higher uptake values, but the problem of desorption from CO₂-swollen PMP could not be avoided and appears to be

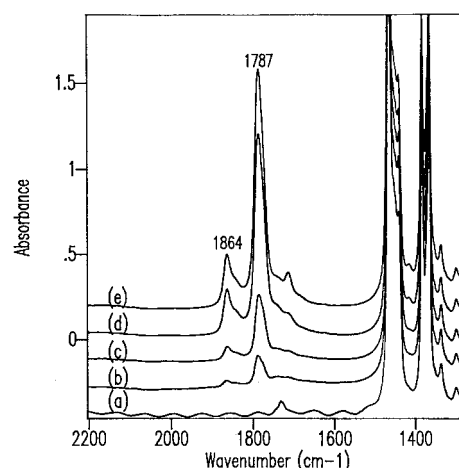


Figure 2. IR spectra of PMP-*g*-MAH after reaction at 125 °C, 400 atm CO₂ for (a) 0, (b) 0.5, (c) 1, (d) 5, and (e) 18 h.

the limiting factor in achieving reasonable uptake values. We believe both from these data and from maleation experiments with variable soaking times that the MAH partitions rapidly into the PMP with a solubility on the order of a few percent.

Determinations of initiator solubility in the substrate under SC CO₂ conditions were also unsuccessful. Uptakes could not be determined by direct gravimetric analysis because of a small substrate mass loss after exposure to the fluid. This mass loss was observed in the uptake experiment even after a SC CO₂ extraction was performed. Use of TGA was not a viable option since the thermal initiator dissociates and reacts with the substrate as temperature is increased. An NMR analysis was attempted on the basis of dissolution of the substrate material after exposure to the initiator/fluid solution, but this resulted in undetectable levels of initiator after lengthy dissolution and analysis at elevated temperatures, as required for PMP solvation.

Maleation. Infrared analysis proved to be a useful method for following the maleation reaction. Figure 2 shows a series of infrared spectra of PMP samples maleated for different time periods. The intensity of the anhydride peaks at 1787 and 1864 cm⁻¹, which correspond to the symmetric and asymmetric C=O stretching of the carbonyl,²⁰ clearly increase with reaction time. The unreacted PMP film contains a peak at 1740 cm⁻¹ (likely a ketone resulting from autoxidation) that is insignificant relative to the anhydride bands. The spectra are normalized to the 1410–1310 cm⁻¹ region of the spectrum associated with the methyl groups of the substrate.

To quantitate the degree of anhydride incorporation in the PMP, a calibration curve was constructed that relates elemental analysis results with those of FTIR (Figure 3). The two sets of data shown compare the determination of oxygen in the sample by direct pyrolysis and by indirect combustion analyses (where it is assumed that the only elements contained in the samples are carbon, hydrogen, and oxygen). The abscissa of this graph is the ratio of the anhydride region to the methyl bend region of the FTIR spectrum, as mentioned above. The combustion analysis proved to be more consistent, having a better least-squares fit to the curve. In addition, the pyrolysis tests yielded data that were rather close to the lower detection limit of the analysis (0.5 wt % oxygen). These factors led to the

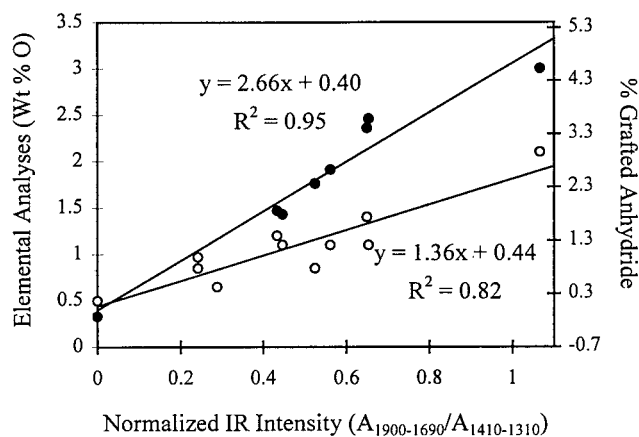


Figure 3. Calibration curves for PMP maleations relating elemental analysis results of oxygen content from (●) combustion and (○) pyrolysis to FTIR results.

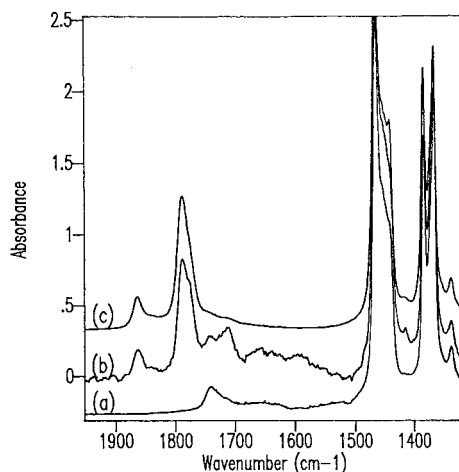


Figure 4. ATR IR spectra of (a) virgin PMP and (b) PMP-*g*-MAH. (c) Transmission IR spectrum of PMP-*g*-MAH.

decision to use the combustion curve as the calibration curve for quantifying PMP maleations. The secondary *y*-axis of Figure 3 indicates the molar percentage of succinic anhydride units grafted relative to PMP repeat units determined using the combustion data. We emphasize that the degree of maleation is much larger in these samples than is observed in commercially maleated linear low-density polyethylene samples. Values of less than 1.2 mol % were determined from elemental analyses by combustion for the commercial samples that we obtained. Without the aid of NMR (which is not feasible due to the presence of cross-links), we could not determine whether the grafted anhydride exists as single or oligomeric units.¹³

With an accurate means of quantifying the maleations, the first issue we addressed was whether this heterogeneous maleation is surface-selective. Figure 4 indicates that the free-radical grafting in SC CO₂ is indeed a bulk, non-surface-selective reaction. This assessment is made by comparing the peak intensities of the 1787 cm⁻¹ symmetric anhydride stretching band in spectra of a sample analyzed by both transmission and ATR IR. The transmission spectrum represents the composition of the entire thickness of the 50 μm grafted film while the ATR IR spectrum assesses only the outermost 1–2 μm of the sample. The peaks due to the anhydride are of nearly identical height, with the transmission spectrum indicating a slightly higher

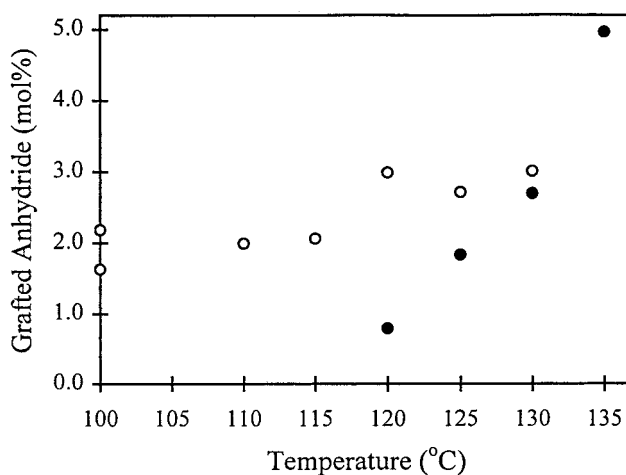


Figure 5. Effect of temperature on the degree of maleation using (○) BPO (4 h soak, 24 h reaction) and (●) DCP (2 h soak, 1 h reaction) as initiators with a 60 °C soak, [MAH] = 0.25 M, [initiator] = 0.04 M, and 180 atm CO₂ pressure (at 60 °C).

degree of maleation (even after running an ATR correction to adjust the spectrum for the dependence of the signal on wavelength). The peak seen at 1710 cm⁻¹ is assigned to carboxylic acids that form as the result of hydrolysis of the anhydride, which is expected considering the surface was in contact with air. The presence of this peak accounts for the lower intensity of the anhydride peak in the ATR IR spectrum. Also shown is the ATR IR spectrum of the unreacted PMP film. The peak due to oxidation is more pronounced than in the transmission spectrum (Figure 2a), which is expected for a surface oxidation.

Controlling Parameters. Below, a comparison is made between the two initiators, BPO and DCP, which have both been explored as initiators for maleation reactions in other systems. Jois and Harrison^{1a} reported that when comparing initiator efficiency in MAH grafting reactions, DCP is a much better choice than BPO; 2,2'-azobis(isobutyronitrile) (AIBN), another initiator, is the least effective. Preliminary studies in our labs with AIBN as well as those with DCP and BPO are in agreement with their findings. In addition, the half-lives of these initiators are quite different. At 125 °C, the reaction temperature used in the SC CO₂ maleation reactions, the half-lives are orders of magnitude apart with AIBN decomposing within a few seconds, BPO within minutes, and DCP requiring hours. AIBN was found to be an inadequate initiator for our system and will not be discussed beyond what is mentioned here.

The effect of temperature on the maleation reactions was explored as a screening experiment to determine the ideal reaction temperature for these systems. Figure 5 illustrates the effect. It should be emphasized that the BPO reactions were run over a 24 h time period to allow for complete reaction of the initiator at all temperatures, while for the DCP reactions, a 1 h reaction was allowed. Temperature seems to have little to no effect on the extent of maleation in the case of the BPO-initiated reactions. The absence of a temperature dependence is likely due to the fact that reactions were run to complete initiator depletion. Assuming that there are no competing side reactions with higher or lower activation energies, temperature independence would be expected. The scatter in the data is most likely

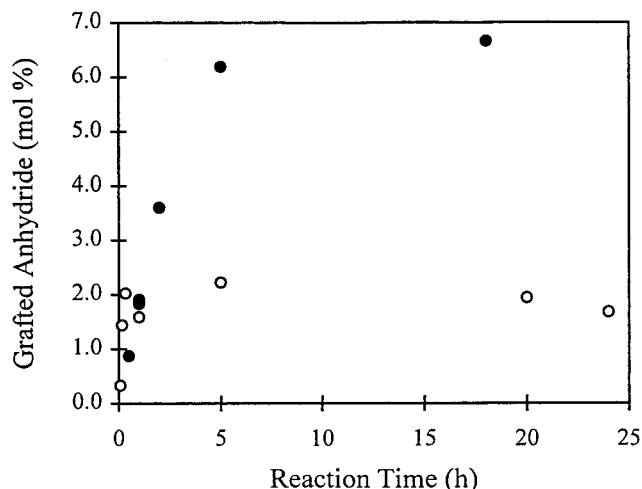


Figure 6. Kinetics of the SC CO₂ maleation reaction at 125 °C, 400 atm using (●) DCP (2 h soak, [MAH] = 0.25 M) and (○) BPO (4 h soak, [MAH] = 0.5 M) as initiators with a 60 °C soak and [initiator] = 0.04 M.

a result of the partial solubility of the initiator in the fluid at lower temperatures, because the BPO does not fully dissolve in the fluid until a temperature above 120 °C is reached. In the DCP-initiated reactions, however, control can be exercised. The long half-life plays a significant role in this case. It should be noted that at temperatures above and including 130 °C for both initiating systems, the samples begin to flow, making analysis more difficult. Due to the physical limitations of running these reactions at higher temperatures and the desire to optimize the maleation as much as possible, the decision was made to run all subsequent reactions at 125 °C.

An analysis of the reaction kinetics for the two initiators reveals that the BPO-initiated reaction is complete within 30 min at 125 °C while for the DCP system, the reaction continues even after 5 h (Figure 6). This again relates to the half-life difference between these species, but the fact that the grafting in the DCP reactions plateaus at a much higher degree of maleation reveals the greater effectiveness of this initiator over BPO. Thus, along with temperature, time can be used to exercise a large degree of control over these reactions.

It is expected¹ that with increased initiator concentration, the percentage of grafting should increase. While Figure 7 concurs with this expectation, plateaus are observed in these experiments at higher concentrations. This is likely because the initiator efficiency decreases as a result of the greater concentration of radicals generated at a given time and/or the fluid-swollen PMP becomes saturated with initiator at some concentration such that increasing initiator concentration in the fluid has no effect on the concentration in the fluid-swollen polymer. The latter explanation is supported by swelling experiments (see below) that indicate the degree of cross-linking of the films increases and then plateaus with increased initiator concentration. We note that there is a difference in the reaction conditions for the two initiator systems graphed. In the case of the DCP data, the reactions were run for only 2 h (see Figure 6), while the BPO data were acquired using samples that had been reacted for 1 h (completion). The figure, therefore, serves only as a comparison of trends within each data set. The error bars on the DCP data are the result of an error analysis study

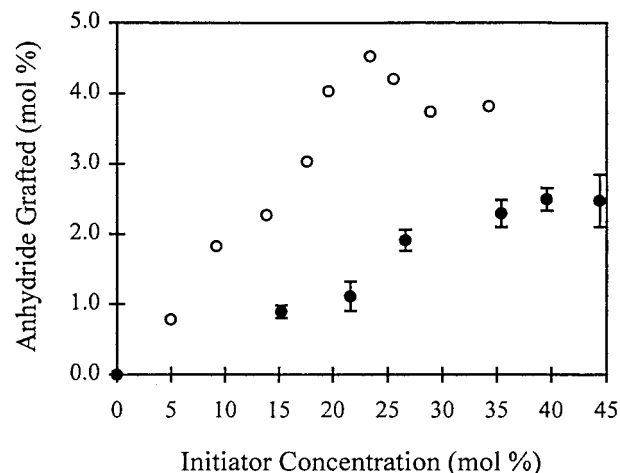


Figure 7. Effect of initiator concentration (relative to MAH) on SC CO₂ maleations using (○) BPO (4 h soak, 1 h reaction, [MAH] = 0.25 M) and (●) DCP (no soak, 2 h reaction, [MAH] = 0.06 M) as initiators with a 60 °C soak and a 125 °C reaction at 400 atm CO₂.

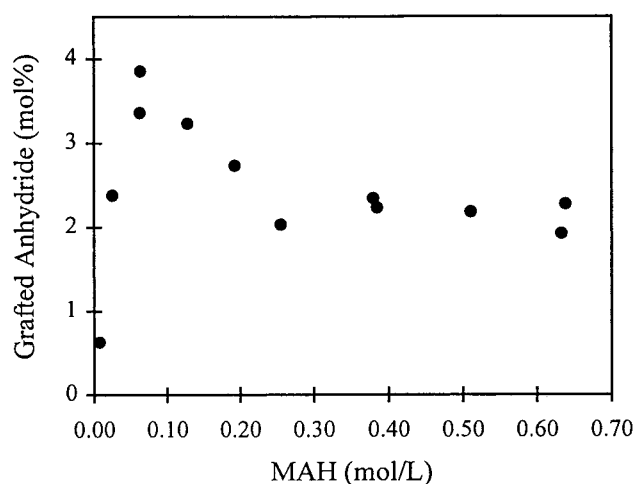


Figure 8. Effect of [MAH] on DCP-initiated reactions with a 2 h reaction at 125 °C, [DCP] = 0.04 M, and 430 atm CO₂.

conducted on these samples. They represent the standard deviation of 4–8 infrared spectra taken at random points along the films.

As with initiator concentration, increasing the MAH content shows an increase in grafting, but, as shown in Figure 8, the effect appears to maximize and then decrease to a lower plateau. The initial upward trend can be explained by an increase in the concentration of anhydride in the PMP and the plateau by a saturation argument as with the experiments varying the initiator concentration. We can provide no explanation, however, for the observation of a maximum in the data. This maximum at 0.63 M corresponds to an initiator concentration of 40 mol % relative to MAH, which is the value of onset of the plateau in Figure 7. The data, therefore, suggests that to optimize maleation, a 3:2 molar ratio (MAH:DCP) should be used.

The effect of CO₂ density on the maleations is not overly pronounced. Figure 9 reveals that the grafting percentage increases to a maximum and then decreases with increasing pressure. This behavior is expected due to the changing solubility parameter of SC CO₂ with pressure.⁸ At lower densities, the fluid phase is expected to dissolve to a lesser extent in the PMP substrate, while at higher pressures, the fluid becomes

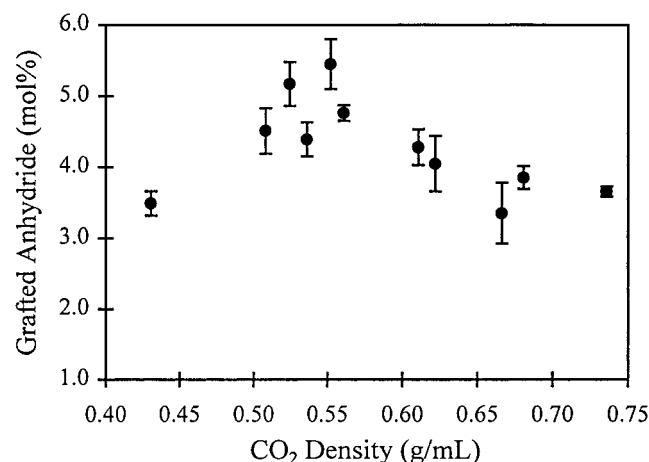


Figure 9. Effect of CO_2 density on the amount of anhydride grafted for DCP-initiated reactions with a 2 h reaction at 125 $^\circ\text{C}$, $[\text{MAH}] = 0.06 \text{ M}$, and $[\text{DCP}] = 0.04 \text{ M}$.

a very good solvent for the reactants, causing them to preferentially partition into the fluid phase over that of the fluid-swollen polymer. The resulting maximum in the curve at 0.55 g/mL (280 atm) indicates a balance of these competing effects.

Several SC CO_2 maleations were conducted on substrates other than PMP. Screening reactions with linear low-density polyethylene produced results similar to the PMP data. Maleation was also briefly explored with a fluorinated polymer to improve its adsorption properties. While the degree of maleation was quite small, the poly(trifluoroethylene) sample showed a marked increase in its adsorption behavior toward inorganic surfaces.

Characterization. As a means of further characterizing the maleation of PMP in SC CO_2 , an analysis of the crystalline portion of the grafted polymer was carried out to determine whether the maleation reaction affects the crystalline regions. PMP is a unique polymer in that at ambient conditions, the crystalline phase is less dense than the amorphous. At temperatures above 58 $^\circ\text{C}$ at ambient pressure, the crystalline phase becomes the more dense.²¹ With the idea that the crystalline regime is rather open, we were interested in determining whether the maleation affected it in some way. Previous studies in our group^{2,4} have shown that the crystalline phase of other substrates is unaltered in SC CO_2 , blend-forming, modification reactions.

DSC analysis (Figure 10) revealed that upon maleation, the crystallinity dropped slightly (from 27% to 24%) but recovered upon second heating. Two distinct endotherms emerged from the initial broad peak of the substrate material upon maleation: one broad peak at lower melting temperature and a much sharper peak with a melting point nearly identical to virgin PMP. The separation of the initial endotherm into two peaks could be the result of the formation of a new crystalline phase (PMP is known to be polymorphic) or to the creation of two distinct populations of more and less perfect crystals of the same overall unit cell. To ascertain which of these explanations is most viable, X-ray analyses were conducted. From d spacing calculations, the virgin and maleated PMP samples were found to contain the same unit cell—a 7_2 helix in a tetragonal packing array. These results support the latter explanation with the crystalline structure being disrupted slightly during maleation, creating a population of less perfect or

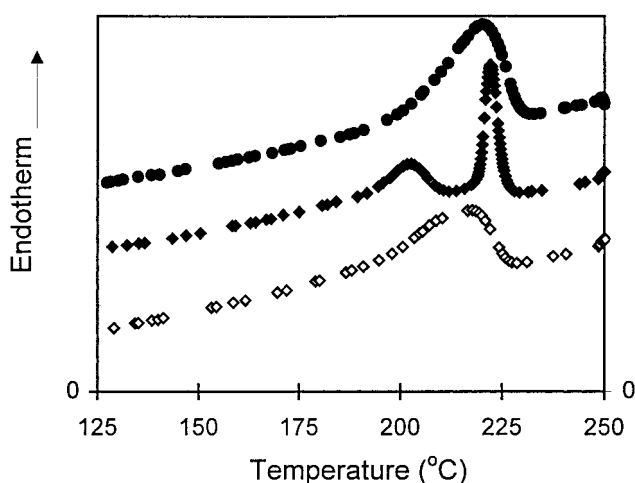


Figure 10. DSC data for (●) unreacted PMP, (◆) PMP-*g*-MAH, and (◇) PMP-*g*-MAH second heating.

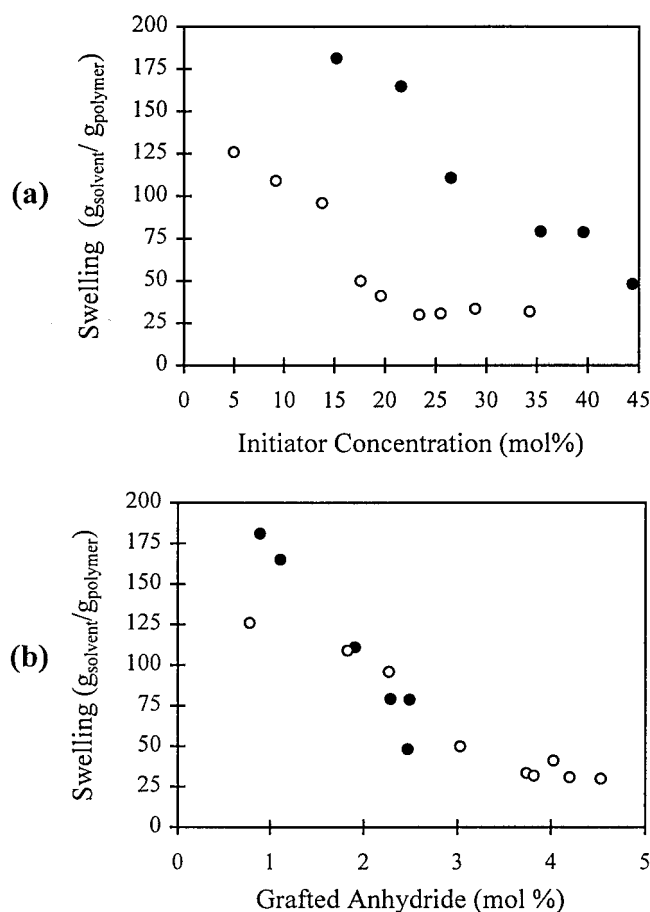


Figure 11. Swelling of insoluble portions of PMP-*g*-MAH samples as a function of (a) initiator concentration (relative to MAH) and (b) anhydride grafted using (●) DCP and (○) BPO as initiators under the reaction conditions listed in Figure 7.

smaller crystals. A control experiment was run that involved exposure of a PMP sample to the supercritical reaction conditions in the absence of reactants. A slight sharpening of the endotherm was observed without the creation of a lower melting peak or a change in the degree of crystallinity.

While the degree of maleation can be easily controlled with the proper choice of initiator, temperature, and time, there is a drawback to this system. As with many polyolefin maleation reactions, especially extruder male-

ations, cross-linking can be a competing reaction. In the case of increasing initiator concentration, it was expected that along with increased maleation, increased cross-linking would result. As shown in Figure 11, this is indeed the case. The cross-linking was gauged using swelling experiments with carbon tetrachloride as the swellant. With higher degrees of cross-linking, the insoluble gel is less able to swell with solvent. In these samples, a decrease is observed in the swelling that corresponds to increasing cross-link density with increasing amounts of initiator present in the reaction. The plateau, which is especially pronounced in the BPO data beginning at 23 mol %, is attributed to a plateau in the concentration of BPO in the SC CO₂-swollen PMP, as mentioned above. The discrepancy in the DCP and BPO data is a result of differing degrees of maleation, as illustrated in the collapsed graph also shown in Figure 11. This indicates that the degree of cross-linking is independent of initiator identity. The cross-links are assumed to be caused by radical-radical combination during the formation of the maleated polymer; however, it is possible that the insolubility is a result of physical cross-linking brought about by polar anhydride-anhydride interactions. Attempts to dissolve the insoluble portions of the maleated polymer samples in a carbon tetrachloride/dimethylacetamide solution proved unsuccessful, suggesting that the cross-links are not completely of polar origin.

Conclusions

By varying time and temperature, the maleation of poly(4-methyl-1-pentene) was effectively controlled in supercritical carbon dioxide. The optimum temperature for these reactions was found to be 125 °C, which allows for rapid reaction without significant sample deformation. A comparison of two initiating systems was made throughout this study, showing dicumyl peroxide to be the more effective reagent compared to benzoyl peroxide. An MAH:DCP molar ratio of 3:2 was found to optimize the degree of maleation. The primary drawback to these reactions is the occurrence of substrate cross-linking, which is independent of the initiator used but dependent on the degree of maleation at a given temperature. The crystalline phase of PMP was not significantly altered by this reaction. The primary advantages of using SC CO₂ to conduct maleation reactions of substrate materi-

als include the ability to control the degree of maleation in bulk samples without the need for efficient extruder mixing or solution processing.

Acknowledgment. We thank the Office of Naval Research and the NSF-sponsored Materials Research Science and Engineering Center for financial support.

References and Notes

- (1) See for example: (a) Jois, Y. H. R.; Harrison, J. B. *J. Macromol. Sci., Rev Macromol. Chem. Phys.* **1996**, *C36* (3), 433. (b) Naqvi, M. K.; Choudhary, M. S. *J. Macromol. Sci., Rev Macromol. Chem. Phys.* **1996**, *C36* (3), 601. (c) Chung, T. C., Ed. *New Advances in Polyolefins*; Plenum Press: New York, 1993.
- (2) Watkins, J. J.; McCarthy, T. J. *Macromolecules* **1995**, *28*, 4067.
- (3) Watkins, J. J.; McCarthy, T. J. *Macromolecules* **1994**, *27*, 4845.
- (4) Kung, E.; Lesser, A. J.; McCarthy, T. J. *Polymer Prepr. (Am. Chem. Soc., Div. Polym. Chem.)* **1997**, *38* (2), 462.
- (5) Rajagopalan, P.; McCarthy, T. J. *Polymer Prepr. (Am. Chem. Soc., Div. Polym. Chem.)* **1997**, *38* (2), 678.
- (6) Watkins, J. J.; McCarthy, T. J. *Chem. Mater.* **1995**, *7*, 1991.
- (7) Hyatt, J. A. *J. Org. Chem.* **1984**, *49*, 5097.
- (8) McHugh, M. A.; Krukons, V. J. *Supercritical Fluid Extraction: Principles and Practice*; Butterworth: Boston, 1984.
- (9) Dispenza, C.; Filardo, G.; Silvestri, G. *Colloid Polym. Sci.* **1997**, *275*, 390.
- (10) Jobling, M.; Howdle, S. M.; Poliakoff, M. *J. Chem Soc., Chem. Commun.* **1990**, 1762.
- (11) Yalpani, M. *Polymer* **1993**, *34*, 1102.
- (12) Heinen, W.; Rosenmöller, C. H.; Wenzel, C. B.; de Groot, H. J. M.; Lugtenburg, J.; van Duin, M. *Macromolecules* **1996**, *29*, 1151.
- (13) De Roover, B.; Sclavons, M.; Carlier, V.; Devaux, J.; Legras, R.; Momtaz, A. *J. Polym. Sci., Polym. Chem. Ed.* **1995**, *33*, 829.
- (14) Heinen, W.; van Duin, M.; Rosenmöller, C. H.; Wenzel, C. B.; de Groot, H. J. M.; Lugtenburg, J. *ANTEC '97* **1997**, 2017.
- (15) Zoller, P.; Starkweather, H. W.; Jones, G. *J. Polym. Sci., Polym. Phys. Ed.* **1986**, *24*, 1451.
- (16) Berens, A. R.; Huvar, G. S.; Korsmeyer, R. W.; Kunig, F. *W. J. Appl. Polym. Sci.* **1992**, *46*, 231.
- (17) Paulaitis, M. E.; Alexander, G. C. *Pure Appl. Chem.* **1987**, *59*, 61.
- (18) Crank, J. *The Mathematics of Diffusion*, 2nd ed.; Oxford University Press: New York, 1975.
- (19) Puleo, A. C.; Paul, D. R.; Wong, P. K. *Polymer* **1989**, *30*, 1357.
- (20) Samay, G.; Nagy, T.; White, J. L. *J. Appl. Polym. Sci.* **1995**, *56*, 1423.
- (21) Tanigami, T.; Yamaura, K.; Matsuzawa, S.; Miyasaka, K. *Polym. J.* **1986**, *18*, 35.

MA980292C